Thickness optimization of Mo films for Cu(InGa)Se_2 solar cell applications

Li Wei(李 微)[a)b)†], Zhao Yan-Min(赵彦民)[a)], Liu Xing-Jiang(刘兴江)[a)],
Ao Jian-Ping(敖建平)[c)], and Sun Yun(孙 云)[c)]

[a)] *National Key Laboratory of Power Sources, Tianjin Institute of Power Sources, Tianjin* 300381, *China*
[b)] *School of Material Science and Engineering, Tianjin University, Tianjin* 300071, *China*
[c)] *Institute of Photoelectronic Thin Film Devices and Technology, Nankai University, Tianjin* 300071, *China*

(Received 26 October 2010; revised manuscript received 9 December 2010)

Mo thin films are deposited on soda lime glass (SLG) substrates using DC magnetron sputtering. The Mo film thicknesses are varied from 0.08 μm to 1.5 μm to gain a better understanding of the growth process of the film. The residual stresses and the structural properties of these films are investigated, with attention paid particularly to the film thickness dependence of these properties. Residual stress decreases and yields a typical tensile-to-compressive stress transition with the increase of film thickness at the first stages of film growth. The stress tends to be stable with the further increase of film thickness. Using the Mo film with an optimum thickness of 1 μm as the back contact, the Cu(InGa)Se_2 solar cell can reach a conversion efficiency of 13.15%.

Keywords: Mo film, Cu(InGa)Se_2, back contact

PACS: 81.15.Cd, 61.10.Nz, 81.15.Ef **DOI:** 10.1088/1674-1056/20/6/068102

1. Introduction

$CuInSe_2$ (CIS) and its gallium alloy Cu(InGa)Se_2 (CIGS)-based solar cell with a Mo/CIGS/ CdS/ZnO structure has emerged as one of the most efficient thin film solar cells.[1,2] Molybdenum is one of the most important materials used as a back contact for CIS solar cells, because of its high melting temperature and low resistivity.[3−5] In a CIS solar cell, Mo film not only provides the electrical properties of an Ohmic contact, but also serves as part of the substrate during the CIS (or CIGS) film growth. Like other refractory metals, Mo film is typically deposited by DC sputtering on glass, thereby ideally providing an inexpensive, inert and mechanically durable substrate.

Stress is always present in each thin film, even though the film is not externally loaded. The quantification of stress and strain in thin films has been an important issue for many years[6,7] because the adverse effects of stress and strain can lead not only to undesirable properties of the thin film structures, but also to the reduced performance of the device.

The structure and stress of a deposited film is strongly influenced by its thickness. As a result, changing the film thickness can induce a significant change in the properties of the grown film. In this work, we focus on the film thickness dependence of stress and structural properties. We find a close correlation between the microstructure and stress of Mo film. The films are subjected to compressive stress with a dense microstructure and exhibit tensile stress with an open porous microstructure. CIGS solar cells are also fabricated using Mo films as the back contact to evaluate optimum film photovoltaic characteristics.

2. Experimental procedures

Mo films were deposited on 4.2 cm × 4.4 cm soda lime glass substrates by DC planar magnetron sputtering. The cathode electrode (Mo target) was 20.4 cm × 5.4 cm × 1 cm in size, 8 cm far from the substrates. When the base pressure was lower than 3×10^{-3} Pa, Ar (99.999%) was introduced into the deposition chamber. The DC sputtering power was kept at 130 W. Prior to deposition, the target was cleaned by "pre-sputtering" for 2 min. The thicknesses of the Mo films were controlled to be in a range from 0.08 μm to 1.5 μm by adjusting sputtering time and measuring their surface profilers.

A CIGS absorption layer was deposited by the 'three-stage' process described earlier.[8−11] In the first stage, In, Ga and Se were co-evapourated at about 350 °C. Subsequently, the substrate heater power was increased up to a growth temperature of about

†Corresponding author. E-mail: cliwei618@126.com
© 2011 Chinese Physical Society and IOP Publishing Ltd

540 °C and Cu and Se were co-evapourated onto the $(In, Ga)_2Se_3$ precursor layer. In the final stage, the additional In, Ga and Se were deposited, with the heater power kept constant.

The crystallographic properties and residual stresses of the grown films were examined by a Philips X'Pert diffractometer with Cu K_α radiation. The film thicknesses were measured by a surface profiler (AMBIOS XP-2). The surface morphologies of the Mo films were observed by a JEOL JSM-6700 field emission scanning electron microscope (FE-SEM). The current density–voltage (J–V) measurement of the cell with a total area 0.87 cm^2 was performed under the standard AM1.5 spectrum for 100 mW/cm^2 irradiance at room temperature.

3. Results

The X-ray diffraction (XRD) patterns of Mo films with different thicknesses are shown in Fig. 1. All Mo films show (110) and (211) diffraction peaks, indicating that each of them has a polycrystalline structure with a (110) preferential orientation perpendicular to the substrate. It can be also seen that crystallization is better for the thicker films, which can be confirmed by comparing the full widths at half maximum of I(110) and I(211).

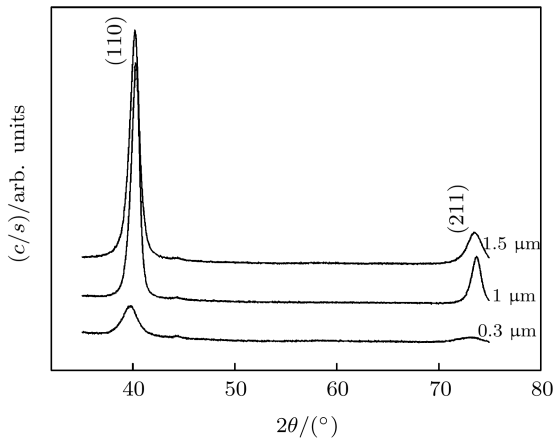


Fig. 1. The XRD patterns of deposited Mo films of different thicknesses.

The residual stress in the Mo films were measured by XRD using the Rocking and Fixed Incidence Multiplane (FIM) techniques. In XRD stress measurement, the strain, $\varepsilon_{\phi\psi}$, is defined as the difference in d spacing between the unstressed and stressed lattice. The residual stress in the film, σ, is calculated for a particular (hkl) plane by the strain

$$\begin{aligned}\varepsilon_{\phi\psi} &= \frac{\Delta d}{d} \\ &\approx \frac{d_{\phi\psi} + d_0}{d_0} \\ &= -\cot\theta_0 \Delta\theta \\ &= -\frac{\cot\theta_0}{2}(2\theta_{\phi\psi} - 2\theta_0)\end{aligned}$$

as

$$\begin{aligned}\sigma &= \frac{E}{1+\upsilon} \times \frac{\partial \varepsilon_{\phi\psi}}{\partial \sin^2\psi} \\ &= -\frac{E}{2(1+v)} \cot\theta_0 \frac{\pi}{180^\circ} \times \frac{\Delta 2\theta_{\phi\psi}}{\Delta \sin^2\psi},\end{aligned}$$

where $d_{\phi\psi}$ and $\theta_{\phi\psi}$ are the lattice spacing and the diffraction angle of (hkl) plane tilted by ψ and rotated by ϕ within the film plane and d_0 and θ_0 are the lattice spacing and diffraction angle of the unstressed lattice. The terms E and v are the Young's modulus of the matrix and the Poisson ratio, respectively. To calculate the residual stress in a film, a number of independent X-ray runs with different ψ angles are performed and then the residual stress is obtained from the slope of the $\varepsilon_{\phi\psi}$ or $d_{\phi\psi}$ versus $\sin^2\Psi$ plot. This technique is called the $\sin^2\Psi$ technique and is commonly used to measure residual stress in films.[12,13]

Using XRD stress measurement techniques, it was found that the stresses in Mo films are strongly related to the deposition thickness. Figure 2 shows that residual stress decreases and yields a typical tensile-to-compressive stress transition with the increase of film thickness at the first stages of film growth. When the film is around 0.6-μm thick, the stress tends to be stable and has less variation with film thickness further increasing. The stress in the growth process obeys[14,15]

$$\sigma = \left[\frac{(2\gamma_{\mathrm{s-v}} - \gamma_{\mathrm{gg}})E(1+v)}{(1-v)/L}\right]^{1/2},$$

where E is the Young's modulus of the matrix, v is its Poisson ratio and L is the length of the island unit.

The stress is very high at the beginning of the growth of the Mo film, which is caused by a mass of crystalline defects and the formation of hillocks and whiskers on the film surface. The stress of the Mo film is dominated by the bending energy of solid–vapor $\gamma_{\mathrm{s-v}}$ which shows a form of tensile stress. The absolute stress rapidly decreases with the increase of film thickness within the first 0.08 μm–0.4 μm and achieves a minimum at about 0.4 μm. The bending energy of solid–vapor $\gamma_{\mathrm{s-v}}$ decreases while the bending energy of grain–grain γ_{gg} increases with the growth of

Mo film, therefore the film shows a compressive stress form. With the further increase of thickness, a slow relaxation takes place and reduces the absolute value of the change in film stress, which is related to the growth process of the film.[16−18] When the film thickness reaches 0.6 μm, in the case of epitaxial or preferentially oriented grain growth, the stress reaches a steady value in the Mo film.

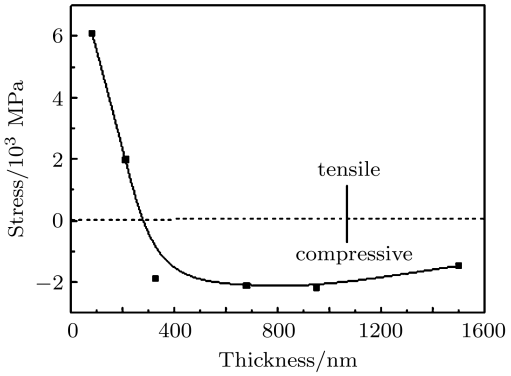


Fig. 2. Residual stress of Mo film as a function of thickness.

The surface morphologies of Mo films with different thicknesses are indicative of evolving microstructures at various stages of film growth. Figure 3 shows the SEM micrographs of a series of Mo films with different thicknesses deposited in the growth stage. The above-mentioned stress variations with film thickness seem to be well related to the growth morphologies of the Mo films, as shown in Fig. 3.

For the thinnest film (as shown in Fig. 3(a)), the structure is characterized by a honeycomb morphology and randomly oriented crystallites. Correspondingly, there is a residual tensile stress in each of these films. The film with an intermediate thickness, as indicated in Fig. 3(b), clearly exhibits significantly elongated grains. In each of these films, the residual stress is compressive. The elongation of the grains appears to saturate for about 1 μm of Mo film thickness. With a further increase in thickness, as shown in Fig. 3(c), the grains are more densely packed and their surfaces become faceted.[19,20] Accompanied by these morphological characteristics, the residual stress in the films tends to be zero.

Resistance decreases with the thickness of the Mo thin film increasing, as shown in Fig. 4. The resistivity decreases to a minimum of 7×10^{-5} Ω·cm at about 1 μm.

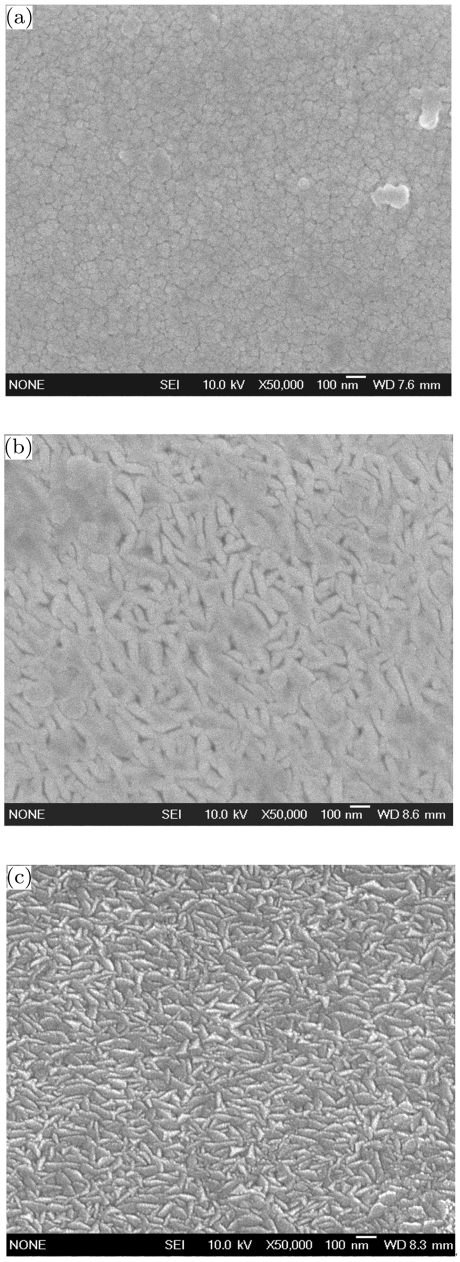


Fig. 3. The scanning electron microscope (SEM) micrographs of deposited Mo films with a thickness of (a) 0.3 μm, (b) 1.0 μm, and (c) 1.5 μm.

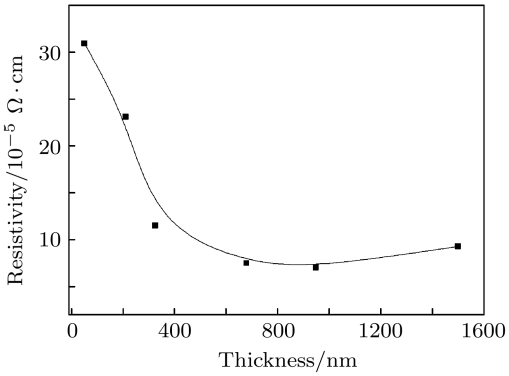


Fig. 4. Resistivity as a function of Mo thickness.

Table 1 shows the performances of the same batch of CIGS solar cells fabricated on the Mo thin films with different thicknesses, without antireflective coating and with a total area of 0.87 cm^2/cell. The compositions of some CIGS thin films each with a thickness of 1.38 μm were measured by XRF and the values of the Cu/In/Ga/Se ratio in the CIGS films are all 23.21/18.04/7.94/50.80 with Ga/(In+Ga)=0.31. The cell corresponding to sample A2 has the highest average efficiency of 13.15% in cells corresponding to all of the samples. It appears that an open-grain structure of Mo film possesses the best open-circuit voltage V_{oc} of 589 mV, the short-circuit current density J_{sc} of 34.22 mA/cm^2 and the fill factor of 65.2%.

Table 1. Performances of the CIGS solar cells for the selected samples.

Sample ID	Thickness/μm	V_{oc}/mV	J_{sc}/(mA/cm^2)	FF/(%)	η/(%)
A1	0.3	515	24.9	44.5	6.57
A2	1.0	589	34.2	65.2	13.15
A3	1.5	570	30.1	64.2	11.04

In this application, it is essential to deposit the Mo film with relatively low stress and relatively low resistivity in order to achieve high adherence and good contact. The cell corresponding to sample A1 has lower efficiency because of the high resistivity of the thinner Mo film. In the film with a thickness of 1.5 μm, the grains are more densely packed and their surfaces became faceted, which prevents Na diffusion from the SLG substrate into the absorber CIGS layer in the second stage of the deposition process where the temperature goes up to about 540 °C. Na diffusion is advantageous during CIGS growth because it leads to a better film morphology and higher conductivity.[21−25] The porosity of around 1.0 μm thick Mo film with good contact and an open-grain structure is conducible to Na diffusion, so the highest efficiency of the device is obtained to be 13.15%. More detailed investigation of the Na diffusion is in progress.

4. Conclusion

In this paper, we present the relation between stress and microstructure in a sputter-deposited Mo film, which can be illustrated by studying the thickness change at the early stages of film growth. The thickness of the Mo film is optimized for its application in a CIGS solar cell. It is found that the Mo film with an optimal thickness of 1 μm acts as an appropriate substrate for growing CIGS film by co-evapouration. The CIGS–Mo bilayer shows good contact and low stress and the CIGS solar cell exhibits a best conversion efficiency of 13.15%.

References

[1] Ramanathan K and Miguel A C 2003 *Photovoltaics Res. Appl.* **11** 225

[2] Ward J S, Ramanathan K, Hasoon F S, Coutts T J, Keane J, Contreras M A, Moriarty T and Noufi R 2002 *Photovoltaics Res. Appl.* **10** 41

[3] Granath K, Rockett A, Bodegard M, Nender C and Stolt L 1995 13th *European Photovoltaic Solar Energy Conference*, October 23–27 Nice, France, p. 1983

[4] Gordillo G, Grizalez M and Hernandez L C 1998 *Solar Energy Materials and Solar Cells* **51** 327

[5] Li W, Ao J P, He Q, Liu F F, Li F Y, Li C J and Sun Y 2007 *Acta Phys. Sin.* **56** 5009 (in Chinese)

[6] Hudson C and Somekh R E 1996 *J. Vac. Sci. Technol.* A **14** 2169

[7] Kamminga J D, Keijser T H, Delhez R and Mittemeijer E J 1998 *Thin Solid Films* **317** 169

[8] Kohara N, Negami T, Nishitani M and Wada T 1995 *Jpn. J. Appl. Phys.* **34** L1141

[9] Wada T, Kohara N, Nishiwaki S and Negami T 2001 *Thin Solid Films* **387** 118

[10] Zhang L, He Q, Xu C M, Xue Y M, Li C J and Sun Y 2008 *Chin. Phys.* B **17** 3138

[11] Xu C M, Sun Y, Li F Y, Zhang L, Xue Y M, He Q and Liu H T 2007 *Chin. Phys.* **16** 788

[12] Sarioglu C, Demirler U, Kursat K M and Urgen M 2005 *Surface & Coatings Technology* **190** 238

[13] Vink T J, Somers M A J, Daams J L C and Dirks A G 1991 *J. Appl. Phys.* **70** 4301

[14] Dietrich E W, Robert B G and Tang L H 1985 *Surf. Sci.* **162** 114

[15] Hofman D W and Gaerttner M R 1980 *J. Vac. Sci. Technol.* **17** 425

[16] Lee H W, Lau S P, Wang Y G, Tay B K and Hng H H 2004 *Thin Solid Films* **458** 15

[17] Sakaguchi K, Iwasa S and Yoshino Y 1998 *Vacuum* **51** 677

[18] Chang J F, Shen C C and Hon M H 2003 *Ceramics International* **29** 245

[19] Chen G F, Yan W B, Chen H J, Cui H Y and Li Y X 2009 *Chin. Phys.* B **18** 2988

[20] Chen G F, Yan W B, Chen H J, Li X H and Li Y X 2009 *Chin. Phys.* B **18** 293

[21] Rockett A, Britt J S, Gillespie T, Marshall C, Al Jassim M M, Hasoon F, Matson R and Basol B 2000 *Thin Solid Films* **372** 212

[22] Bodeg M, Granath K and Stolt L 2000 *Thin Solid Films* **361–362** 9

[23] Lyahovitskaya V, Feldman Y, Gartsman K, Cohen H, Cytermann C and Cahen D 2002 *J. Appl. Phys.* **91** 4205

[24] Schroeder D J and Rockett A A 1997 *J. Appl. Phys.* **82** 4982

[25] Schuler S, Siebentritt S, Nishiwaki S, Rega N, Beckmann J, Brehme S and Lux-Steiner M C 2004 *Phys. Rev.* B **69** 045210